$\mathcal{PT}$-symmetry breaking in multilayers with resonant loss and gain locks light propagation direction

Denis V. Novitsky[1,2,3],[*] Alina Karabchevsky[4,5,6], Andrei V. Lavrinenko[7],
Alexander S. Shalin[2], and Andrey V. Novitsky[7,8]

[1] *B. I. Stepanov Institute of Physics, National Academy of Sciences of Belarus,*
Nezavisimosti Avenue 68, 220072 Minsk, Belarus
[2] *ITMO University, Kronversky Prospekt 49, 197101 St. Petersburg, Russia*
[3] *Saint Petersburg Electrotechnical University "LETI",*
5 Prof. Popova Str., 197376 St. Petersburg, Russia
[4] *Electrooptical Engineering Unit, Ben-Gurion University of the Negev,*
David Ben-Gurion Blvd, P.O.B. 653, 8410501 Beer-Sheva, Israel
[5] *Ilse Katz Institute for Nanoscale Science & Technology,*
Ben-Gurion University of the Negev, Beer-Sheva, 8410501, Israel
[6] *Center for Quantum Information Science and Technology,*
Ben-Gurion University of the Negev, Beer-Sheva, 8410501, Israel
[7] *DTU Fotonik, Technical University of Denmark,*
Ørsteds Plads 343, DK-2800 Kongens Lyngby, Denmark
[8] *Department of Theoretical Physics and Astrophysics,*
Belarusian State University, Nezavisimosti Avenue 4, 220030 Minsk, Belarus

Using the Maxwell-Bloch equations for resonantly absorbing and amplifying media, we study the temporal dynamics of light propagation through the $\mathcal{PT}$-symmetric structures with alternating loss and gain layers. This approach allows us to precisely describe the response of the structure near the exceptional points of $\mathcal{PT}$-symmetry breaking phase transition and, in particular, take into account the nonlinear effect of loss and gain saturation in the $\mathcal{PT}$-symmetry broken state. We reveal that in this latter state the multilayer system possesses a lasing-like behavior releasing the pumped energy in the form of powerful pulses. We predict locking of pulse direction due to the $\mathcal{PT}$-symmetry breaking, as well as saturation-induced irreversibility of phase transition and nonreciprocal transmission.

I. INTRODUCTION

$\mathcal{PT}$-symmetric structures and $\mathcal{PT}$-symmetry breaking seem to be one of the most intensively studied fields in optics and photonics of active systems [1–3]. It dates back to the seminal works of Bender and Boettcher [4, 5], who discovered the real-valued spectra of non-Hermitian Hamiltonians in quantum mechanics provided these Hamiltonians are parity-time ($\mathcal{PT}$) symmetric, i.e., invariant with respect to simultaneous parity change and time reversal. Such ideas can be straightforwardly transferred to optics using the spatial ordering of passive and active components, thus introducing the concept of an optical $\mathcal{PT}$-symmetric system.

The simplest optical $\mathcal{PT}$-symmetric structure can be realized by means of one-dimensional multilayers — similar to photonic crystals — with proper spatial variation of the complex permittivity as $\varepsilon(z) = \varepsilon^*(-z)$ (here asterisk stands for complex conjugation). This condition implies that the real part of the permittivity or refractive index is an even function of the coordinate, whereas the imaginary part is an odd function. Change of the sign of the imaginary part of the permittivity $\mathrm{Im}\varepsilon(z) = -\mathrm{Im}\varepsilon(-z)$ apparently requires amplifying materials. It can be, for instance, an alternation of loss and gain in periodic multilayers. Two principal schemes, longitudinal and trans- verse ones, are usually employed. In the former system, light propagates directly through the multilayer. In the latter scheme light propagates perpendicularly to the permittivity distribution, along the layers boundaries, being analogous to a system of interconnected waveguides (an optical grating). First theoretical [6, 7] and experimental [8] results on optical $\mathcal{PT}$ symmetry were reported exactly for the coupled waveguides.

$\mathcal{PT}$ symmetry allows new ways for controlling radiation fluxes both in optics and plasmonics [9]. A number of effects can be highlighted as a fingerprint of the $\mathcal{PT}$ symmetry: nonreciprocity of light transmission and beam power oscillations [7], anisotropic transmission resonances [10], unidirectional "invisibility" [11], negative refraction, and focusing of light [12]. $\mathcal{PT}$ symmetry governs light localization in disordered structures [13]. The usage of gain media raises questions concerning available nonlinear phenomena, such as optical switching and generation of new types of solitons [14, 15]. Apodization of the refractive index spatial profiles can be used to facilitate switching conditions in $\mathcal{PT}$-symmetric Bragg gratings [16]. Some nonlinear effects connected to $\mathcal{PT}$ symmetry have been recently observed in experiments with coherent atomic gases [17]. More prospects are opened by the fact that $\mathcal{PT}$-symmetric optical gratings are capable of supporting topologically protected bound states [18].

It should be noted that the effects mentioned above may be observable in loss-gain structures lacking the $\mathcal{PT}$-

symmetry. A typical example is the reflectionless transmission and unidirectional "invisibility" for both normal [19, 20] and oblique [21] incidence. However, the symmetry breaking at the exceptional points belongs exclusively to the $\mathcal{PT}$ symmetry domain.

There is a number of phenomena associated with violation of the $\mathcal{PT}$ symmetry. First, a sharp change in polarization response of the system is possible at the exceptional points [22]. Later an omnipolarizer was designed for converting any light polarization into a given one [23]. Second, enhanced sensitivity of such kind of systems to external perturbations near exceptional points provides a new approach for sensing [24, 25]. Third, $\mathcal{PT}$-symmetry breaking plays an important role in laser physics offering new types of lasers [26–28] and anti-lasers [29] based on the effect of coherent perfect absorption [30, 31]. Finally, the possibility of light stopping at the exceptional point was recently reported [32].

In this paper, we study the phenomenon of $\mathcal{PT}$-symmetry breaking in one-dimensional multilayers composed of resonantly absorbing and amplifying media. We describe propagation of light in the time domain using the Maxwell-Bloch equations and taking into account loss and gain saturation. The influence of the saturable nonlinearity on nonreciprocity and bistability of $\mathcal{PT}$-symmetric structures was previously reported both for transverse [33] and longitudinal geometries [34–37]. However, those investigations introduced the saturation phenomenologically via the permittivity. Our approach is based on self-consistent description of temporal dynamics for both light field and medium loss/gain exhibiting a more realistic treatment of $\mathcal{PT}$-symmetric optical systems. Therefore, we have a deep insight into peculiarities of the $\mathcal{PT}$-symmetry breaking and related effects. In particular, we study the lasing-like regime in the $\mathcal{PT}$-symmetry broken state, where the saturation effects lead to the unique phase transition in the parameter space and nonreciprocal transmission of generated pulses. Pulse-direction locking by the $\mathcal{PT}$-symmetry breaking in the lasing-like regime is related to the strong light confinement and resembles light polarization locking to its propagation direction in quantum optics [38].

The paper is organized as follows. Section II is devoted to the description of the theoretical model of the loss-gain multilayer and parameters used in calculations. We discuss light behavior in the $\mathcal{PT}$-symmetric phase in Sec. III by comparing numerical solution of the Maxwell-Bloch equations and stationary transfer-matrix calculations. In Sec. IV, the $\mathcal{PT}$-symmetry breaking as a phase transition to the lasing-like regime is studied with emphasis on temporal dynamics of the light propagating through the multilayers. Section V summarizes the article.

II. RESONANT LOSS AND GAIN MEDIA

A periodic planar structure composed of $2N$ alternating loss and gain layers shown in Fig. 1 is illuminated
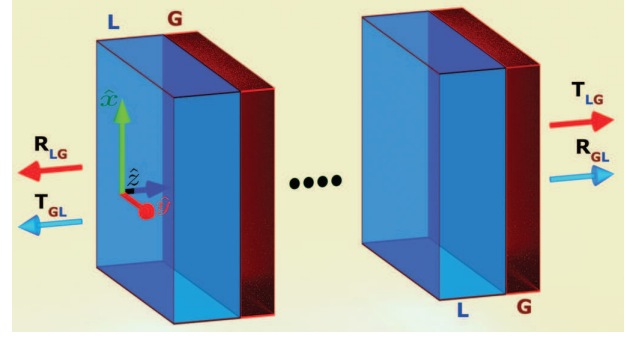

FIG. 1. N-periods multilayer system of alternating slabs with loss (L) and gain (G). Transmissions and reflections and corresponding propagation directions are indicated for the waves incident from left-hand (T_{LG} and R_{LG}) and right-hand (T_{GL} and R_{GL}) sides.

by monochromatic light of angular frequency ω at normal incidence. In this study, both loss and gain are described in the similar manner, using the model of a homogeneously-broadened two-level medium. Excluding the rapidly varying factors $\exp(-i\omega t)$ in polarization, population difference, and electric field, we write the Maxwell-Bloch equations [39] for slowly varying amplitudes of these quantities as

$$\frac{d\rho}{d\tau} = il\Omega w + i\rho\delta - \gamma_2\rho, \tag{1}$$

$$\frac{dw}{d\tau} = 2i(l^*\Omega^*\rho - \rho^* l\Omega) - \gamma_1(w - w_{eq}), \tag{2}$$

$$\frac{\partial^2\Omega}{\partial\xi^2} - n_d^2\frac{\partial^2\Omega}{\partial\tau^2} + 2i\frac{\partial\Omega}{\partial\xi} + 2in_d^2\frac{\partial\Omega}{\partial\tau} + (n_d^2 - 1)\Omega$$
$$= 3\alpha l\left(\frac{\partial^2\rho}{\partial\tau^2} - 2i\frac{\partial\rho}{\partial\tau} - \rho\right), \tag{3}$$

where $\tau = \omega t$ and $\xi = kz$ are respectively the dimensionless time and distance, $\Omega = (\mu/\hbar\omega)A$ is the normalized Rabi frequency, A is the electric field strength, ω is the light circular frequency, $k = \omega/c$ is the wavenumber in vacuum, c is the speed of light, $\hbar$ is the reduced Planck constant, and μ is the dipole moment of the quantum transition. Rabi frequency is dynamically coupled to the characteristics of the two-level system – complex amplitude of microscopic (atomic) polarization ρ and difference between populations of ground and excited states w. Efficiency of the light-matter coupling is given by the dimensionless parameter $\alpha = \omega_L/\omega = 4\pi\mu^2 C/3\hbar\omega$, where ω_L is the Lorentz frequency and C is the concentration (density) of active (two-level) atoms. In general, light frequency ω is detuned from frequency ω_0 of the atomic resonance as described by $\delta = (\omega_0 - \omega)/\omega$. The normalized relaxation rates of population $\gamma_1 = 1/(\omega T_1)$ and polarization $\gamma_2 = 1/(\omega T_2)$ are expressed by means of the longitudinal T_1 and transverse T_2 relaxation times. The influence of the polarization of the background dielectric having real-valued refractive index n_d on the embedded active particles is taken into account by the local-field

enhancement factor $l = (n_d^2 + 2)/3$ [40, 41].

Equilibrium population difference w_{eq} will allow us to describe both gain and loss materials with the same Maxwell-Bloch equations (1)-(3). When external pump is absent, the two-level atoms are in the ground state ($w_{eq} = 1$), and the medium is lossy. In the case of gain, the equilibrium population difference can be referred to as a pumping parameter. In the fully inverted medium, all atoms are excited by the pump ($w_{eq} = -1$). For the saturated medium with both levels populated equally in the equilibrium, there are no transitions between the levels ($w_{eq} = 0$).

In the steady-state approximation, when the amplitudes of population difference, polarization, and field are time-independent, one can use the effective permittivity of a two-level medium [21]

$$\varepsilon_{eff} = n_d^2 + 4\pi\mu C\rho_{st}/E = n_d^2 + \frac{K(-\delta + i\gamma_2)}{1 + |\Omega|^2/\Omega_{sat}^2}, \quad (4)$$

where $\Omega_{sat} = \sqrt{\gamma_1(\gamma_2^2 + \delta^2)/4l^2\gamma_2}$ sets the level of saturation intensity and $K = 3\omega_L l^2 w_{eq}/[\omega(\gamma_2^2 + \delta^2)]$. At the exact resonance $\delta = 0$ and in approximation of low-intensity external radiation $|\Omega| \ll \Omega_{sat}$, Eq. (4) transforms to $\varepsilon_{eff} \approx n_d^2 + 3il^2\omega_L T_2 w_{eq}$. From this equation it is clear that gain and loss correspond to negative and positive w_{eq}, respectively. In the stationary approximation, it is straightforward to obtain a $\mathcal{PT}$-symmetric structure composed of alternating layers with balanced loss (ε_{eff+}) and gain (ε_{eff-}), where

$$\varepsilon_{eff\pm} \approx n_d^2 \pm 3il^2\omega_L T_2|w_{eq}|. \quad (5)$$

$\mathcal{PT}$ symmetry holds true, because the necessary condition $\varepsilon(z) = \varepsilon^*(-z)$ is fulfilled, providing even (odd) function of z for the real (imaginary) part of the permittivity. In Supplemental Material [42], $\mathcal{PT}$-symmetry conditions are derived straight from the Maxwell-Bloch equations. It is shown that the system is $\mathcal{PT}$-symmetric only in a steady state established after some transient period.

Identity of the absolute values of the imaginary parts of permittivities ε_{eff+} and ε_{eff-} can be achieved in different ways. From a practical point of view, it would be convenient to take unexcited absorbing layers ($w_{eq,L} = 1$) and pump only the amplifying layers to the level $w_{eq,G} = -\alpha_L/\alpha_G$, where α_L and α_G are the light-matter coupling coefficients for loss and gain layers, respectively. Tuning of these coefficients can be properly carried out by affecting the concentration of active particles in both types of layers. Without imposing any restrictions, it is fair to claim within this theoretical investigation that the loss and gain layers have equal concentrations C (hence, equal couplings α) and absolute values of the pumping parameter $|w_{eq}|$. Some additional data on the variant with completely unexcited absorbing layers are given in Supplemental Material [42].

Eqs. (1)–(3) are solved numerically using the FDTD approach developed in our previous publication [43] and recently adapted to study loss-gain structures [21]. As

an initial value of the population difference, we employ the pumping parameter, i.e., $w(t = 0) = w_{eq}$. Comparison of the results of numerical simulations with those of the transfer-matrix method with Eq. (5) for permittivities of loss and gain layers will unveil the limitations of applicability of the latter approach.

In this paper, we use semiconductor doped with quantum dots as an active material and assume the condition of exact resonance $\delta = 0$ is valid. It can be characterized by the following parameters [44, 45]: $n_d = 3.4$, $\omega_L = 10^{11}$ s^{-1}, $T_1 = 1$ ns, and $T_2 = 0.5$ ps. Gain coefficient $g = 4\pi\text{Im}(\sqrt{\varepsilon_{eff-}})/\lambda \le 10^4$ cm^{-1} is estimated according to Eq. (5) for $\lambda \sim 1.5$ μm and $|w_{eq}| \le 0.2$ can be realized in practice [46]. The multilayer structure contains $N = 20$ unit cells. Both loss and gain layers have the same thickness $d = 1$ μm. The pumping scheme similar to that realized by Wong et $al.$ [29] can be used in our system. It is also worth noting that the choice of materials is not unique, but the multilayer parameters and light wavelength may need to be appropriately adjusted to obtain similar results with different materials.

III. TEMPORAL DYNAMICS OF LIGHT IN $\mathcal{PT}$-SYMMETRIC PHASE

We start our study analysing the stationary characteristics of one-dimensional $\mathcal{PT}$-symmetric structures. In the stationary mode, the transfer-matrix method for the wave propagation through multilayers with permittivities (5) is exploited. Owing to reciprocity of the system, the transmission of oppositely propagating (forward and backward) waves is the same, but the reflection is different. We denote these two directions of wave propagation with subscripts LG and GL (see Fig. 1) originating from the order of layers in the unit cell of the structure. In the case of $w_{eq} = 0$ (homogeneous dielectric slab of thickness $2Nd$), the reflections are equal, $R_{LG} = R_{GL}$ [Fig. 2(a)]. Divergence of the curves for R_{LG} and R_{GL} in Figs. 2(b)-2(d) indicates existence of the $\mathcal{PT}$-symmetry in the full accordance with the properties of transfer matrices of such systems [10]. In these figures, one can notice another well-known feature – the so-called anisotropic transmission resonance (ATR) [10]. It emerges under the following conditions: transmission $T = 1$ and one of the reflections is zero. Thus, the ATR arises for the two wavelengths marked with arrows in Fig. 2 corresponding to $R_{GL} > R_{LG} = 0$ and $R_{LG} > R_{GL} = 0$. Transmission exceeds unity between these points.

The increase of the pumping parameter (hence, the absolute value of the imaginary part of slabs' permittivities) results in the red shift of the ATR. This means that the ATR can be reached by changing $|w_{eq}|$ at any fixed wavelength near the transmission peak. In order to examine this prediction of the transfer-matrix method, we perform numerical simulations of the Maxwell-Bloch equations (1)-(3) for a monochromatic wave ($\lambda = 1.513$ μm) propagating through the $\mathcal{PT}$-symmetric multilayer
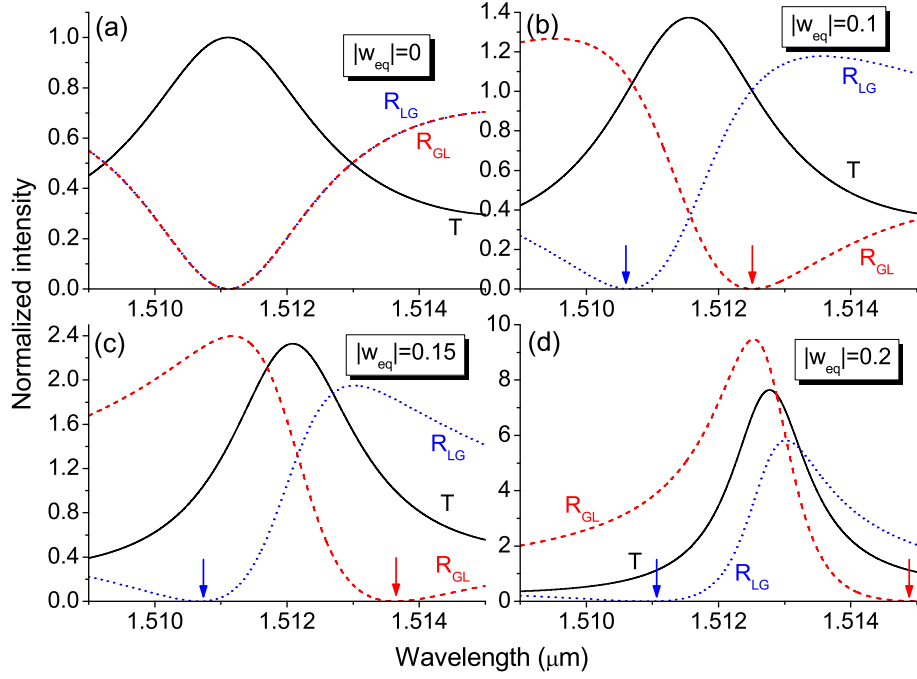
FIG. 2. Reflection (R) and transmission (T) spectra for different levels of pumping: (a) $|w_{eq}| = 0$, (b) $|w_{eq}| = 0.1$, (c) $|w_{eq}| = 0.15$, and (d) $|w_{eq}| = 0.2$. The parameters of the $\mathcal{PT}$-symmetric structure are given in the text. Arrows mark anisotropic transmission resonances.
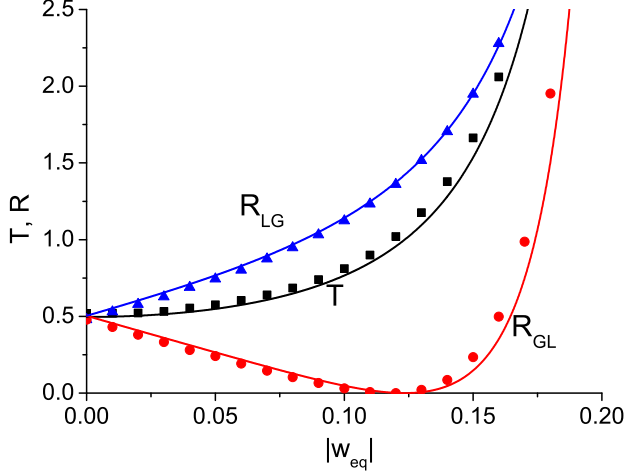

FIG. 3. Dependence of stationary levels of the reflection (R) and transmission (T) on pumping parameter $|w_{eq}|$ at the wavelength $\lambda = 1.513$ μm. Symbols and lines correspond to results of numerical and transfer-matrix calculations, respectively.

with different pumping parameters. To keep the correspondence with the transfer-matrix approach, the saturation should be neglected. Here it is realized for as low incident wave amplitude as $\Omega_0 = 10^{-5}\gamma_2 \ll \Omega_{sat}$. The results of numerical calculations shown with symbols in Fig. 3 agree well with those of matrix method (lines in Fig. 3). The ATR at $|w_{eq}| \sim 0.125$ is also con-

firmed in the FDTD calculations. Temporal dynamics shown in Fig. 4 demonstrates the transient process to the steady-state formation in the dielectric slab [in the absence of loss and gain, panel (a)] and $\mathcal{PT}$-symmetric structure in conditions of the ATR [panel (b)]. Since the steady state is rapidly established, the transfer-matrix approach is well applicable in this no-saturation regime. Absence of saturation is directly demonstrated by the inset in Fig. 4, where the population difference does not change during establishment of the steady state. The initial transient regime is unavoidable in realistic systems. It can be studied with the FDTD method, and $\mathcal{PT}$ symmetry is unreachable in this mode due to impossibility to change the sign of relaxation rates γ_1 and γ_2 (see Ref. [42]).

IV. PHASE TRANSITION DYNAMICS

$\mathcal{PT}$-symmetry breaking can be considered as a peculiar phase transition. It can be realized either by changing wavelength λ of light for a given value of pumping parameter $|w_{eq}|$, or, conversely, by changing the pumping parameter at a fixed wavelength. The latter variant is analyzed in this paper. The former one deserves a separate study, since it implies the necessity to consider the effects of frequency detuning. The criterion of the $\mathcal{PT}$-symmetry breaking is usually formulated in terms of the eigenvalues s_1 and s_2 of the scattering matrix [10]. The scattering matrix connects the left and right input fields
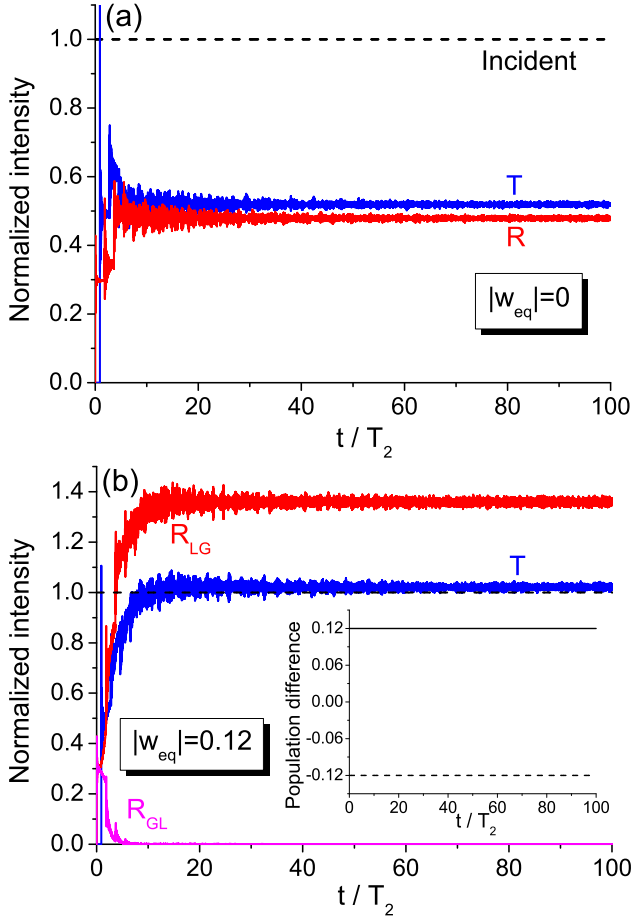
FIG. 4. Temporal dynamics of the reflected (R) and transmitted (T) intensity for the pumping parameters (a) $|w_{eq}| = 0$ and (b) $|w_{eq}| = 0.12$. Inset shows dynamics of population difference at the entrance of the first loss and gain layers.

FIG. 5. (a) Logarithm of eigenvalues s_1 and s_2 and (b) difference of eigenvectors $|\mathbf{v}_1 - \mathbf{v}_2|$ of the scattering matrix as a function of the pumping parameter $|w_{eq}|$.

with left and right output fields. A $\mathcal{PT}$-symmetric system has unimodular eigenvalues $|s_1| = |s_2| = 1$ of the scattering matrix. When $\mathcal{PT}$ symmetry is violated, the modules of the eigenvalues are inverse as $|s_1| > 1$ and $|s_2| = 1/|s_1| < 1$. At the points of phase transition called exceptional points, the eigenvectors of the scattering matrix coincide. Using the definition of the scattering matrix [10]

$$S = \begin{pmatrix} r_{LG} & t_{GL} \\ t_{LG} & r_{GL} \end{pmatrix}, \qquad (6)$$

we calculate both eigenvalues and eigenvectors for pumping parameter $|w_{eq}|$ swept through the whole interval from 0 to 1. Here t_{LG}, t_{GL}, r_{LG}, and r_{GL} are the transmission and reflection coefficients, which can be expressed through the respective elements of transfer matrix M: $t_{LG} = 1/M_{11}$, $t_{GL} = \det[M]/M_{11} = t_{LG}$ (since $\det[M] = 1$), $r_{LG} = M_{21}/M_{11}$, and $r_{GL} = -M_{12}/M_{11}$. Stationary transmission and reflection are calculated as $T = |t_{LG}|^2 = |t_{GL}|^2$, $R_{LG} = |r_{LG}|^2$, and $R_{GL} = |r_{GL}|^2$. Results of transfer-matrix calculations for the multilayer structure with the permittivities (5) are shown in Fig. 5.
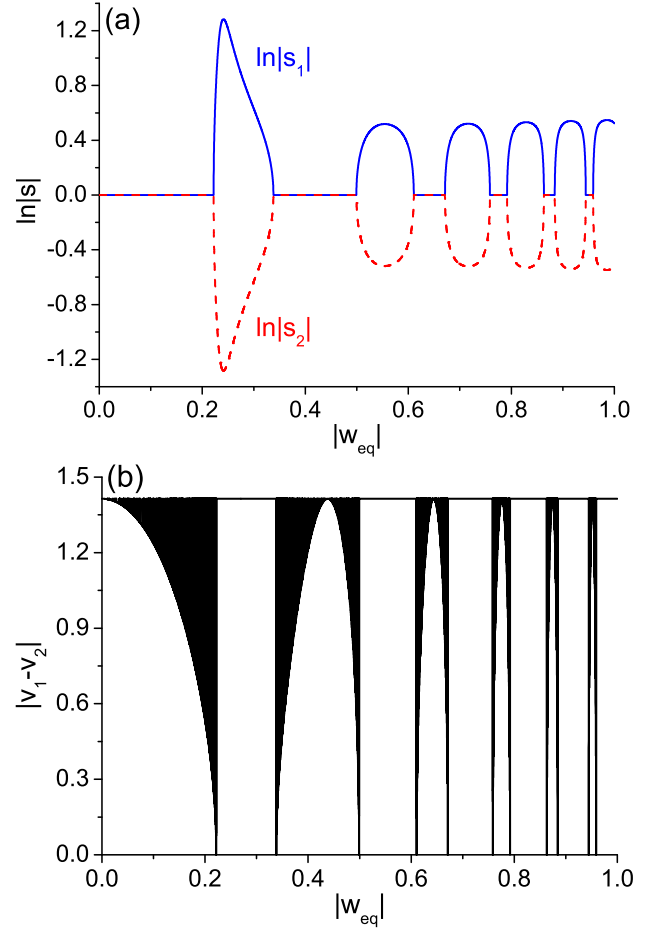
At the first exceptional point $|w_{eq}| \approx 0.222$, the phase transition occurs and eigenvalues cease to be unimodular [Fig. 5(a)], whereas the difference between eigenvectors vanishes [Fig. 5(b)]. Unimodularity is violated and, therefore, $\mathcal{PT}$ symmetry is broken up to the second exceptional point. The latter returns the system into the $\mathcal{PT}$-symmetric state. All in all, there is a number of ranges of $|w_{eq}|$ with broken symmetry and a corresponding number of exceptional points.

Transfer-matrix approach used so far cannot describe dynamics of the wave propagation in resonant media by its definition. Now we will employ the rigorous Maxwell-Bloch equations for studying light dynamics near an exceptional point. There is a dramatic discrepancy between the two calculation techniques, when the pumping parameter approaches the exceptional point. Relative difference in transmission calculated with help of the Maxwell-Bloch and transfer-matrix approaches, $|T_{MB} - T_{TM}|/T_{MB} \approx 0.13$, results in the satisfactory agreement for $|w_{eq}| = 0.22$, but its value 0.48 at $|w_{eq}| = 0.23$ is unacceptably large. Such a large discrepancy stems from the qualitatively different behaviors of the system
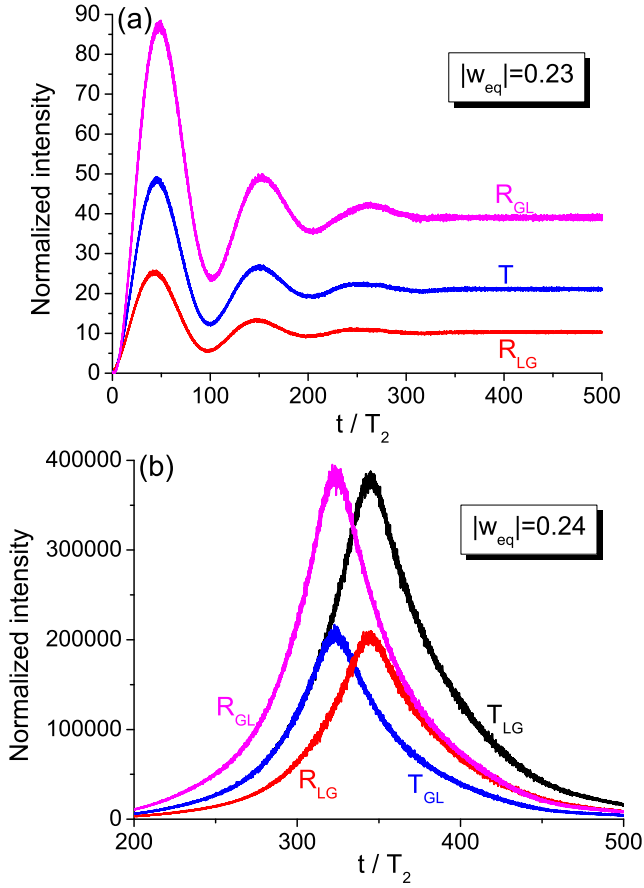
FIG. 6. Temporal dynamics of the reflected (R) and transmitted (T) intensity for the pumping parameter (a) $|w_{eq}| = 0.23$ and (b) $|w_{eq}| = 0.24$.

at $|w_{eq}| = 0.23$: the system is above the exceptional point according to the transfer-matrix method, whereas it is still in the $\mathcal{PT}$-symmetric state according to the FDTD simulations. In fact, temporal dynamics with an established stationary state in Fig. 6(a) is distinctive for the $\mathcal{PT}$ symmetry (cf. Fig. 4). Formation of the steady state after a rather short time corroborates existence of the balance between gain and loss at $|w_{eq}| = 0.23$. The general tendency is that the closer to the exceptional point, the longer the transient period is. At the exceptional point [Fig. 6(b)], the field rapidly grows changing population difference w, this grow being limited by saturation.

Breaking of $\mathcal{PT}$ symmetry is expected to result in the strong (exponential) amplification of propagating waves due to the fact that gain can not be compensated with losses in this case. In Fig. 6(b), instability exhibiting very strong light amplification is observed at $|w_{eq}| = 0.24$. The energy pumped in the system is promptly released as a high-intensity pulse. In concordance with Ref. [21], this regime can be called a lasing-like (or quasilasing) mode. It can be treated as a dynamical feature of the phase state of broken $\mathcal{PT}$ symmetry. In contrast to the true lasing the pulse is generated not by small field

fluctuations, but rather in response to the incident wave (though the intensity of input wave can be taken much lower, as evidenced by Supplemental Material Fig. S4 [42]). At the exceptional point, we have a very long transient period and the stationary levels of reflection and transmission are again expected to occur in the long-time limit [21]. These levels strongly differ from those calculated with the transfer-matrix method due to saturation development discussed further. In other words, the resulting population difference will be no more determined by pumping parameter w_{eq} as assumed in Eq. (5). The pulse gets shorter and more powerful with increasing $|w_{eq}|$ as evidenced by comparison of Fig. 6(b) and Supplemental Material Fig. S1 [42]. The spectra of transmitted radiation shown in Fig. 7 indicate the shift of maximal amplification from the resonant wavelength $\lambda = 1.513$ μm (below the exceptional point) to longer wavelengths (above the exceptional point). This redshift in the lasing-like regime can be explained by two factors: (i) higher light absorption on the resonant wavelength in the loss layers, so that amplification at the neighboring wavelengths becomes prevalent, (ii) intensity modulation due to incomplete stationary-state establishment (see Supplemental Material Fig. S5 [42]). We should stress that although the matrix method with permittivities (5) is able to approximately determine an exceptional point, it fails in adequate description of the phase transition and in describing temporal dynamics of light-structure interaction. In other words, the full system of Maxwell-Bloch equations should be exploited in the vicinity of the points of $\mathcal{PT}$-symmetry breaking.

Strong amplification of a signal in the non-$\mathcal{PT}$-symmetric phase [Fig. 6(b)] plays important role in loss and gain saturation. Indeed, normalized light amplitude Ω inside the system is not much less than Ω_{sat} anymore. Population difference preserves its initial value $w(t) = w_{eq}$ in the $\mathcal{PT}$-symmetric state below the exceptional point (see the dashed lines in Fig. 8, for $|w_{eq}| = 0.23$). However, fluctuations of the population difference due to saturation occur above the exceptional point, at $|w_{eq}| = 0.24$, in both LG (in the loss layer) and GL (in the gain layer) configurations. Saturation imposes constraint on further increase of light intensity as evidenced by the coincidence of the intensity peak in Fig. 6(b) and saturation development in time in Fig. 8. Fluctuations indicate that the $\mathcal{PT}$ symmetry is broken through violation of the necessary condition $\varepsilon(z) = \varepsilon^*(-z)$ and loss and gain are not balanced anymore. Saturation also leads to *the irreversible phase transition* in the system: the return of the system to the $\mathcal{PT}$-symmetric state predicted by the stationary theory at larger pumping parameters (see Fig. 5) is impossible, since Eq. (5) is not valid anymore. Direct FDTD calculations for $|w_{eq}| > 0.24$ (see Supplemental Material Fig. S1 [42]) do support this conclusion resulting in the lasing-like dynamics similar to that shown in Fig. 6(b).

Broken $\mathcal{PT}$ symmetry drastically affects dynamics of the transmitted and reflected waves. Owing to the non-
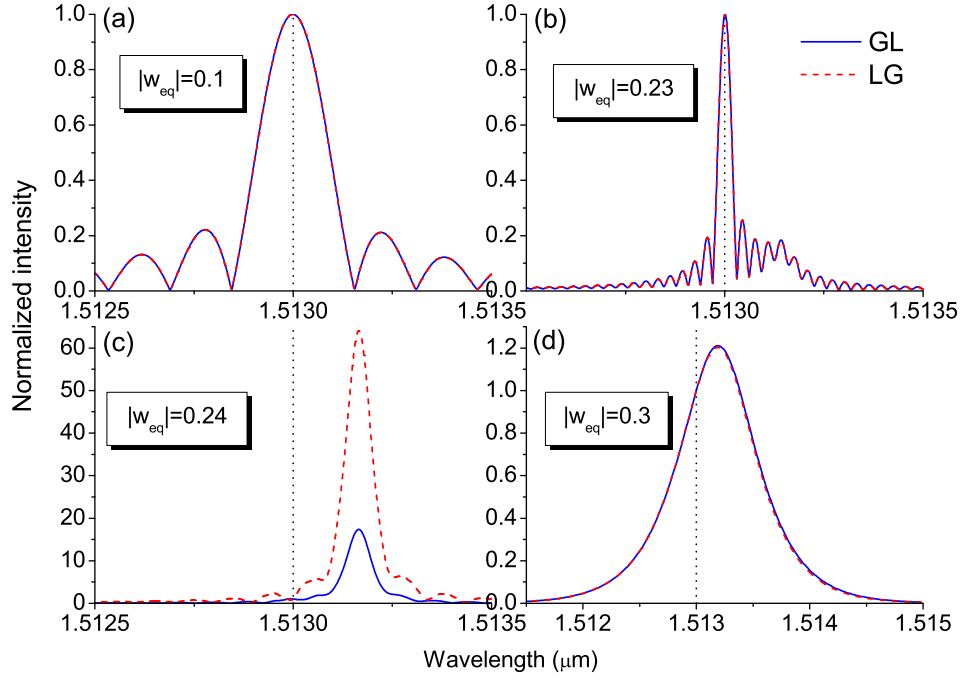
FIG. 7. Spectra of transmitted radiation for different levels of pumping: (a) $|w_{eq}| = 0.1$, (b) $|w_{eq}| = 0.23$, (c) $|w_{eq}| = 0.24$, and (d) $|w_{eq}| = 0.3$. The spectra are normalized on the intensity at the resonant wavelength 1.513 μm.
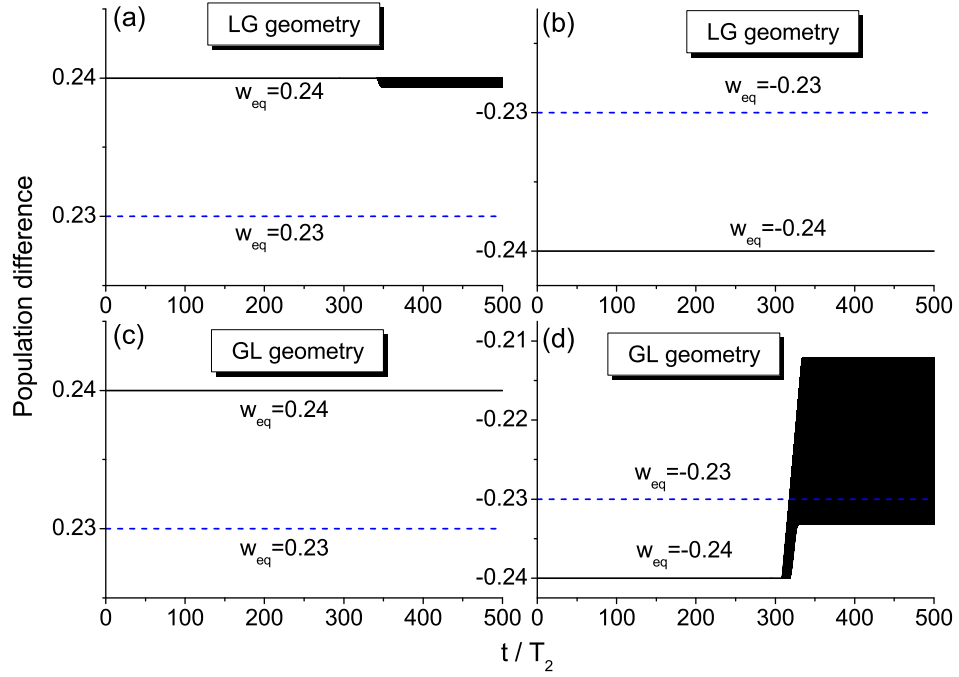

FIG. 8. Temporal dynamics of the population difference in the first unit cell of LG and GL structures at the pumping parameters $|w_{eq}| = 0.23$ and 0.24: (a), (c) $w(t)$ in the loss layer and (b), (d) $w(t)$ in the gain layer.

linear process of saturation, the transmission becomes asymmetric, $T_{LG} \neq T_{GL}$, i.e., the multilayer structure is *nonreciprocal*. Usually the saturation-induced nonreciprocity is introduced through the nonlinear permittivity Eq. (4) [35, 36], but solution of dynamic Eqs. (1)-

(3) is more accurate and informative. In the saturation regime the system is non-Hermitian, but it can be linearized to a $\mathcal{PT}$-symmetric multilayer [36].

Intensities of the pulses escaping the system do not depend on the direction of incident light: almost the
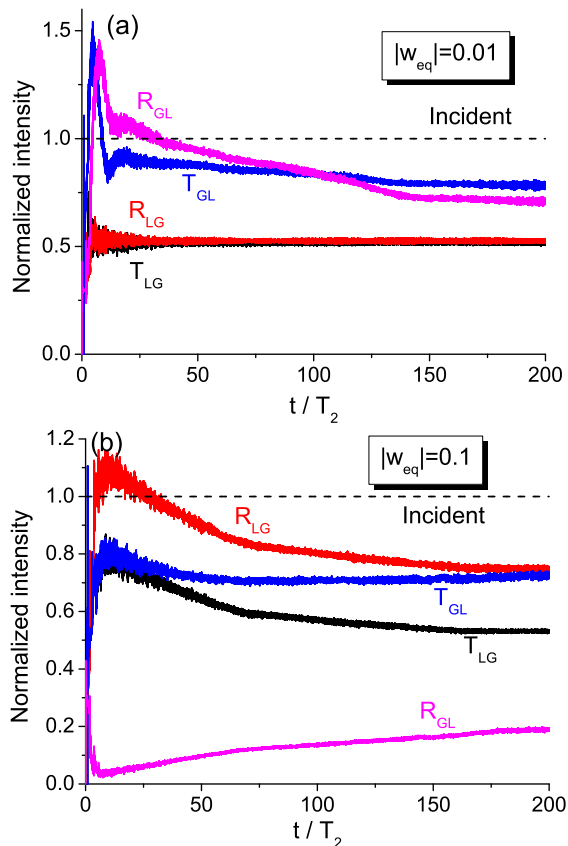
FIG. 9. Temporal dynamics of the reflected (R) and transmitted (T) intensity for the pumping parameter (a) $|w_{eq}| = 0.01$ and (b) $|w_{eq}| = 0.1$ in the case of the wave with relatively large initial amplitude $\Omega_0 = 10^{-2}\gamma_2$.

same pulses are emitted from the gain and loss ends of the multilayer after reversing the input light direction ($T_{LG} = R_{GL}$ and $T_{GL} = R_{LG}$) as shown in Fig. 6(b). In other words, direction of the output pulses is *locked by* $\mathcal{PT}$*-symmetry breaking*. This locking can be presumably caught only within the dynamical calculations, because it has not been reported earlier. Nonreciprocal transmission is accompanied by the propagation direction locking at higher pumping as well, what is demonstrated in Supplemental Material Fig. S1 [42] for $|w_{eq}| = 0.3$ and 0.4. Locking of the light propagation directions can be viewed as a possible basis for peculiar all-optical diodes and transistors.

It should be emphasized that the saturation is not the reason for this locking. In order to demonstrate this, we consider wave propagation in saturation regime (for initial amplitude $\Omega_0 = 10^{-2}\gamma_2$) which breaks $\mathcal{PT}$ symmetry at every value of the pumping parameter. Nonreciprocity of transmission due to saturation is clearly seen in Fig. 9, but the direction locking of output pulses is missing. Therefore, the $\mathcal{PT}$-symmetry breaking is necessary for this locking to occur.

The behavior similar to that described above generally occurs near the exceptional points as evidenced by Figs.

S2, S3, and S4 in Supplemental Material [42]. In particular, the number of layers controls position of the exceptional point: when the structure length is decreased, higher pumping is needed for $\mathcal{PT}$-symmetry breaking (Fig. S2 of Supplemental Material [42]) and vice versa. Although system's response is generally very complex due to interplay of the loss/gain and multilayer resonances [37], the results similar to discussed above are expected for other parameters of the structure and proper operating frequency. Such scalability is encouraging for designing realistic realizations of $\mathcal{PT}$-symmetric multilayers. We would like to emphasize that another model of $\mathcal{PT}$-symmetric multilayer with unexcited absorbing layers mentioned in Section II provides the similar results (see Supplemental Material Fig. S6 [42]).

V. CONCLUSION

We have analyzed temporal dynamics of light in $\mathcal{PT}$-symmetric periodic multilayers, the gain and loss slabs being modeled as a resonant medium. Light-matter interactions in the resonant media are described by the Maxwell-Bloch equations, which are simulated numerically to provide deeper insight into transition dynamics between the $\mathcal{PT}$-symmetric and $\mathcal{PT}$-broken phases. In particular, predictions of the stationary transfer-matrix method are shown to be inadequate in the vicinity of the exceptional points. We feature the so-called lasing-like regime in the $\mathcal{PT}$-symmetry broken state characterized by emission of powerful pulses of radiation and development of saturation. The latter is the reason for phase transition irreversibility – that is, the system cannot return to the $\mathcal{PT}$-symmetric state for the pumping parameters above the exceptional point. In the $\mathcal{PT}$-broken phase, the direction of pulses escaping the system is found to be locked by the $\mathcal{PT}$-symmetry breaking, meaning that the intensities of two output waves are independent of the direction of the incident radiation. The approach based on the Maxwell-Bloch equations seems to be rather general and applicable to structures with other geometries, e.g., coupled ring resonators [26]. We envisage its application to investigation of other effects near the exceptional points, such as coherent perfect absorption (anti-lasing) [29–31]. Intricate interplay between loss and gain in $\mathcal{PT}$-symmetric systems opens up new opportunities for constructing photonic devices for optical communications, computing, and sensing. The approach proposed here is expected to be useful to realize some of these diverse functionalities.

ACKNOWLEDGMENTS

[1] A. A. Zyablovsky, A. P. Vinogradov, A. A. Pukhov, A. V. Dorofeenko, and A. A. Lisyansky, Phys. Usp. **57**, 1063 (2014).

[2] L. Feng, R. El-Ganainy, and L. Ge, Nat. Photon. **11**, 752 (2017).

[3] R. El-Ganainy, K. G. Makris, M. Khajavikhan, Z. H. Musslimani, S. Rotter, and D. N. Christodoulides, Nat. Phys. **13**, 11 (2018).

[4] C. M. Bender and S. Boettcher, Phys. Rev. Lett. **80**, 5243 (1998).

[5] C. M. Bender, Rep. Prog. Phys. **70**, 947 (2007).

[6] R. El-Ganainy, K. G. Makris, D. N. Christodoulides, and Z. H. Musslimani, Opt. Lett. **32**, 2632 (2007).

[7] K. G. Makris, R. El-Ganainy, D. N. Christodoulides, and Z. H. Musslimani, Phys. Rev. Lett. **100**, 103904 (2008).

[8] C. E. Rüter, K. G. Makris, R. El-Ganainy, D. N. Christodoulides, M. Segev, and D. Kip, Nat. Phys. **6**, 192 (2010).

[9] F. Yang and Z. L. Mei, Sci. Rep. **5**, 14981 (2015).

[10] L. Ge, Y. D. Chong, and A. D. Stone, Phys. Rev. A **85**, 023802 (2012).

[11] Z. Lin, H. Ramezani, T. Eichelkraut, T. Kottos, H. Cao, and D. N. Christodoulides, Phys. Rev. Lett. **106**, 213901 (2011).

[12] R. Fleury, D. L. Sounas, and A. Alù, Phys. Rev. Lett. **113**, 023903 (2014).

[13] Ya. V. Kartashov, C. Hang, V. V. Konotop, V. A. Vysloukh, G. Huang, and L. Torner, Laser Photon. Rev. **10**, 100 (2016).

[14] S. V. Suchkov, A. A. Sukhorukov, J. Huang, S. V. Dmitriev, C. Lee, and Yu. S. Kivshar, Laser Photon. Rev. **10**, 177 (2016).

[15] V. V. Konotop, J. Yang, and D. A. Zezyulin, Rev. Mod. Phys. **88**, 035002 (2016).

[16] A. T. Lupu, H. Benisty, and A. V. Lavrinenko, IEEE J. Sel. Top. Quant. Electr. **22**, 4402807 (2016).

[17] C. Hang and G. Huang, Adv. Phys. X **2**, 737 (2017).

[18] S. Weimann, M. Kremer, Y. Plotnik, Y. Lumer, S. Nolte, K. G. Makris, M. Segev, M. C. Rechtsman, and A. Szameit, Nat. Mater. **16**, 433 (2017).

[19] Y. Shen, X. H. Deng, and L. Chen, Opt. Express **22**, 19940 (2014).

[20] J. Ramirez-Hernandez, F. M. Izrailev, and N. N. Makarov, Phys. Rev. A **96**, 013856 (2017).

[21] D. V. Novitsky, V. R. Tuz, S. L. Prosvirnin, A. V. Lavrinenko, and A. V. Novitsky, Phys. Rev. B **96**, 235129 (2017).

[22] M. Lawrence, N. Xu, X. Zhang, L. Cong, J. Han, W. Zhang, and S. Zhang, Phys. Rev. Lett. **113**, 093901 (2014).

[23] A. U. Hassan, B. Zhen, M. Soljacic, M. Khajavikhan, and D. N. Christodoulides, Phys. Rev. Lett. **118**, 093002 (2017).

[24] W. Chen, S. K. Özdemir, G. Zhao, J. Wiersig, and L. Yang, Nature (London) **548**, 192 (2017).

[25] H. Hodaei, A. U. Hassan, S. Wittek, H. Garcia-Gracia, R. El-Ganainy, D. N. Christodoulides, and M. Khajavikhan, Nature (London) **548**, 187 (2017).

[26] L. Feng, Z. J. Wong, R.-M. Ma, Y. Wang, and X. Zhang, Science **346**, 972 (2014).

[27] H. Hodaei, M.-A. Miri, M. Heinrich, D. N. Christodoulides, and M. Khajavikhan, Science **346**, 975 (2014).

[28] Z. Gu, N. Zhang, Q. Lyu, M. Li, S. Xiao, and Q. Song, Laser Photon. Rev. **10**, 588 (2016).

[29] Z. J. Wong, Y.-L. Xu, J. Kim, K. O'Brien, Y. Wang, L. Feng, and X. Zhang, Nat. Photon. **10**, 796 (2016).

[30] Y. D. Chong, L. Ge, H. Cao, and A. D. Stone, Phys. Rev. Lett. **105**, 053901 (2010).

[31] S. Longhi, Phys. Rev. A **82**, 031801(R) (2010).

[32] T. Goldzak, A. A. Mailybaev, and N. Moiseyev, Phys. Rev. Lett. **120**, 013901 (2018).

[33] H. Ramezani, T. Kottos, R. El-Ganainy, and D. N. Christodoulides, Phys. Rev. A **82**, 043803 (2010).

[34] S. Phang, A. Vukovic, H. Susanto, T. M. Benson, and P. Sewell, Opt. Lett. **39**, 2603 (2014).

[35] X. Liu, S. Dutta Gupta, and G. S. Agarwal, Phys. Rev. A **89**, 013824 (2014).

[36] D. R. Barton III, H. Alaeian, M. Lawrence, and J. Dionne, Phys. Rev. B **97**, 045432 (2018).

[37] P. Witoński, A. Mossakowska-Wyszyńska, and P. Szczepański, IEEE J. Quant. Electron. **53**, 2100111 (2017).

[38] P. Lodahl, S. Mahmoodian, S. Stobbe, A. Rauschenbeutel, P. Schneeweiss, J. Volz, H. Pichler, and P. Zoller, Nature (London) **541**, 473 (2017).

[39] D. V. Novitsky, Phys. Rev. A **84**, 013817 (2011).

[40] M. E. Crenshaw, Phys. Rev. A **78**, 053827 (2008).

[41] N. Bloembergen, *Nonlinear Optics* (Benjamin, New York, 1965).

[42] See Supplemental Material at [URL] for derivation of the conditions for $\mathcal{PT}$ symmetry; additional calculations of temporal dynamics of light in $\mathcal{PT}$-symmetry broken phases; calculations for the case of completely unexcited absorbing layers.

[43] D. V. Novitsky, Phys. Rev. A **79**, 023828 (2009).

[44] E. D. Palik (ed.), *Handbook of Optical Constants of Solids* (Academic Press, San Diego, 1998).

[45] J.-C. Diels and W. Rudolph, *Ultrashort Laser Pulse Phenomena* (Academic Press, San Diego, 2nd edn, 2006).

[46] V. E. Babicheva, I. V. Kulkova, R. Malureanu, K. Yvind, and A. V. Lavrinenko, Photon. Nanostruct. – Fund. Appl. **10**, 389 (2012).

Supplemental Material for
$\mathcal{PT}$-symmetry breaking in multilayers with resonant loss and gain locks light propagation direction

Denis V. Novitsky[1,2,3], Alina Karabchevsky[4,5,6], Andrei V. Lavrinenko[7],
Alexander S. Shalin[2], and Andrey V. Novitsky[7,8]

[1] B. I. Stepanov Institute of Physics, National Academy of Sciences of Belarus,
Nezavisimosti Avenue 68, 220072 Minsk, Belarus
[2] ITMO University, Kronversky Prospekt 49, 197101 St. Petersburg, Russia
[3] Saint Petersburg Electrotechnical University "LETI",
5 Prof. Popova Str., 197376 St. Petersburg, Russia
[4] Electrooptical Engineering Unit, Ben-Gurion University of the Negev,
David Ben-Gurion Blvd, P.O.B. 653, 8410501 Beer-Sheva, Israel
[5] Ilse Katz Institute for Nanoscale Science & Technology,
Ben-Gurion University of the Negev, Beer-Sheva, 8410501, Israel
[6] Center for Quantum Information Science and Technology,
Ben-Gurion University of the Negev, Beer-Sheva, 8410501, Israel
[7] DTU Fotonik, Technical University of Denmark,
Ørsteds Plads 343, DK-2800 Kongens Lyngby, Denmark
[8] Department of Theoretical Physics and Astrophysics,
Belarusian State University, Nezavisimosti Avenue 4, 220030 Minsk, Belarus

I. DERIVATION OF THE CONDITIONS FOR $\mathcal{PT}$ SYMMETRY

Let us derive the conditions for $\mathcal{PT}$ symmetry directly from the Maxwell-Bloch equations. We start with the quantum-mechanics-like equation

$$\hat{H}(\mathbf{r},t)\psi(\mathbf{r},t) = \lambda\psi(\mathbf{r},t), \tag{S1}$$

where $\hat{H}$ is a differential operator. It is transformed to

$$\hat{H}^*(-\mathbf{r},-t)\psi^*(-\mathbf{r},-t) = \lambda^*\psi^*(-\mathbf{r},-t), \tag{S2}$$

under the action of parity $\hat{P}$ and time $\hat{T}$ operators. In other words, the $\hat{P}\hat{T}$ operator changes $z \to -z$, $t \to -t$, and $i \to -i$. The system is $\mathcal{PT}$-symmetric, if $\hat{H}(\mathbf{r},t) = \hat{H}^*(-\mathbf{r},-t)$ and $\psi(\mathbf{r},t) = \psi^*(-\mathbf{r},-t)$. Then Eqs. (S1) and (S2) coincide and $\hat{H}$ has a real spectrum $\lambda = \lambda^*$.

Now we turn to the Maxwell-Bloch equations and denote the action of $\hat{P}\hat{T}$-operator with the tilde, e.g., $\tilde{\rho} = \hat{P}\hat{T}\rho(z,t) = \rho^*(-z,-t)$. Acting with the $\mathcal{PT}$ operator on Eqs. (1)-(3) of the main text, one gets

$$\frac{d\tilde{\rho}}{d\tau} = i\tilde{l}\tilde{\Omega}\tilde{w} + i\tilde{\rho}\tilde{\delta} + \gamma_2\tilde{\rho}, \tag{S3}$$

$$\frac{d\tilde{w}}{d\tau} = 2i(\tilde{l}^*\tilde{\Omega}^*\tilde{\rho} - \tilde{\rho}^*\tilde{l}\tilde{\Omega}) + \gamma_1(\tilde{w} - \tilde{w}_{eq}), \tag{S4}$$

$$\frac{\partial^2\tilde{\Omega}}{\partial\xi^2} - \tilde{n}_d^2\frac{\partial^2\tilde{\Omega}}{\partial\tau^2} + 2i\frac{\partial\tilde{\Omega}}{\partial\xi} + 2i\tilde{n}_d^2\frac{\partial\tilde{\Omega}}{\partial\tau} + (\tilde{n}_d^2-1)\Omega$$
$$= 3\tilde{\alpha}\tilde{l}\left(\frac{\partial^2\tilde{\rho}}{\partial\tau^2} - 2i\frac{\partial\tilde{\rho}}{\partial\tau} - \tilde{\rho}\right). \tag{S5}$$

Eq. (S5) coincides with Eq. (3) from the main text, if $n_d = \tilde{n}_d$, $\alpha = \tilde{\alpha}$, $\Omega = \tilde{\Omega}$, and $\rho = \tilde{\rho}$. In other words, $n_d(\xi) = n_d^*(-\xi)$, $\alpha(\xi) = \alpha(-\xi)$, $\Omega(\xi,\tau) = \Omega^*(-\xi,-\tau)$,

and $\rho(\xi,\tau) = \rho^*(-\xi,-\tau)$. Condition $n_d(\xi) = n_d^*(-\xi)$ leads to $l(\xi) = l^*(-\xi)$. The relaxation rates cannot change the sign, therefore, Eqs. (S3) and (S4) cannot be turned into Eqs. (1) and (2) of the main text. Thus, the $\mathcal{PT}$ symmetry is not applicable to the Maxwell-Bloch equations in general, but only to the particular cases of negligible relaxation rates (in comparison with the frequency of light) and/or stationary regime.

In the stationary regime, time-independent Ω, w and ρ can be joined into a vector $\psi(\xi) = (\Omega, \rho, W)^T$, where $W = iw$, and Eqs. (1) and (2) of the main text read

$$l\Omega W + i\rho\delta - \gamma_2\rho = 0,$$
$$l^*\Omega^*\rho - \rho^*l\Omega + \gamma_1(W - iw_{eq}) = 0. \tag{S6}$$

Operator $\hat{P}\hat{T}$ transforms these equations to

$$\tilde{l}\tilde{\Omega}\tilde{W} - i\tilde{\rho}\tilde{\delta} - \gamma_2\tilde{\rho} = 0,$$
$$\tilde{l}^*\tilde{\Omega}^*\tilde{\rho} - \tilde{\rho}^*\tilde{l}\tilde{\Omega} + \gamma_1(\tilde{W} + i\tilde{w}_{eq}) = 0. \tag{S7}$$

PT-symmetry requires $\psi = \tilde{\psi}$, $w_{eq} = -\tilde{w}_{eq}$, and $\delta = -\tilde{\delta}$, or $\psi(\xi) = \psi^*(-\xi)$, $w_{eq}(\xi) = -w_{eq}(-\xi)$, and $\delta(\xi) = -\delta(-\xi)$.

Thus, conditions for existence of $\mathcal{PT}$ symmetry in resonant media are (i) the stationary regime, (ii) $w_{eq}(\xi) = -w_{eq}(-\xi)$, and (iii) $\delta(\xi) = -\delta(-\xi)$. The same conditions follow from Eqs. (4) and (5).

Note also that in the case of the low-intensity incident pulse (as compared to the saturation intensity, $\Omega \ll \Omega_{sat}$), the population difference w remains unchanged and equal to w_{eq}, while the polarization $\rho \sim \Omega$ remains small and rapidly takes the stationary value. Under such conditions, the system remains almost $\mathcal{PT}$-symmetric during all the process of the stationary-state establishment.

II. CALCULATIONS FOR THE CASE DISCUSSED IN THE MAIN TEXT

In this section, we give results of additional calculations which support Section 4 of the main text. Figure S1 shows the profiles of reflected and transmitted intensity for the pumping parameters $|w_{eq}| = 0.3$ and 0.4 at the same parameters as in Fig. 6. These profiles possess the same pattern as in Fig. 6(b), i.e., we see direction locking and nonreciprocity characteristic for the lasing-like regime, but the pulses are much shorter and more smooth. Note that scattering-matrix calculations predict $\mathcal{PT}$-symmetric state at $|w_{eq}| = 0.4$ (see Fig. 5(a)).

In order to prove that the lasing-like regime is connected with $\mathcal{PT}$-symmetry breaking, we calculate wave propagation through the structures with the changed parameters. This change results in the shift of the exceptional point. Figure S2 shows the case of 1.5-times increased density of active particles, so that the Lorentz frequency is $\omega_L = 1.5 \times 10^{11}$ s^{-1}. In this case, $\mathcal{PT}$-symmetry breaking occurs at lower pumping parameters in comparison with the case discussed in the main text. On the contrary, decreasing the number of layers in the structure leads to the shift of the exceptional point to larger $|w_{eq}|$ as seen in Fig. S3 for $N = 15$. In both cases, however, breaking of $\mathcal{PT}$ symmetry is accompanied by the transition to the lasing-like regime with direction locking clearly seen.

We have also studied the case of much lower incident wave amplitude $\Omega_0 = 10^{-10}\gamma_2$ than that considered in the main text ($\Omega_0 = 10^{-5}\gamma_2$). The results for this case shown in Fig. S4 indicate that the position of exceptional point does not depend on initial light intensity and, hence, is the inherent characteristic of the system. *Relative* (or normalized by the incident intensity) transmission and reflection in Fig. S4(a) and Fig. 6(a) are identical in the $\mathcal{PT}$-symmetric state. In the state of broken $\mathcal{PT}$ symmetry, the intensities of transmitted and reflected pulses in Fig. S4(b) and Fig. 6(b) have the same *absolute* (non-normalized) values reached over different periods: the weaker input wave, the longer period.

Finally, Fig. S5 shows the process of steady-state establishment above the exceptional point. One can see that this process is much longer than in the $\mathcal{PT}$-symmetric state and is accompanied by violent fluctuations of intensity, which may be one of the reasons for spectral maximum shift reported in Fig. 7 of the main text.

III. CALCULATIONS FOR THE CASE OF COMPLETELY UNEXCITED ABSORBING LAYERS

This section contains additional information on another possibility to achieve $\mathcal{PT}$ symmetry mentioned in Section 2 of the main text. We take completely unexcited absorbing layers ($w_{eq,L} = 1$) and pump the amplifying layers to a certain level $w_{eq,G} < 0$, which depends on the relationship between densities C of active particles in loss and gain layers (or, equivalently, on the relationship between the light-matter coupling coefficients, since $\alpha \sim C$). Indeed, for the loss layers we have

$$\varepsilon_{eff+} \approx n_d^2 + 3il^2\omega_{L,L}T_2, \tag{S8}$$

whereas for the gain layers we can write

$$\varepsilon_{eff-} \approx n_d^2 - 3il^2\omega_{L,G}T_2|w_{eq,G}|. \tag{S9}$$

The necessary condition for $\mathcal{PT}$ symmetry requires the equality of imaginary parts Eqs. (S8) and (S9), so that $|w_{eq,G}| = \omega_{L,L}/\omega_{L,G} = \alpha_L/\alpha_G$, where α_L and α_G are light-matter coupling coefficients for loss and gain layers, respectively.

The results of calculations with $\omega_{L,G} = 10^{11}$ s^{-1} and $\omega_{L,L} = |w_{eq,G}|\omega_{L,G}$ for $|w_{eq}| = 0.23$ and 0.24 are shown in Fig. S6. The other parameters are the same as in the main text. It is seen that the profiles of transmitted and reflected intensity are in good agreement with that reported in Fig. 6. This proves that the cases of equal particles density and completely unexcited absorbing layers are equivalent for study of $\mathcal{PT}$ symmetry.
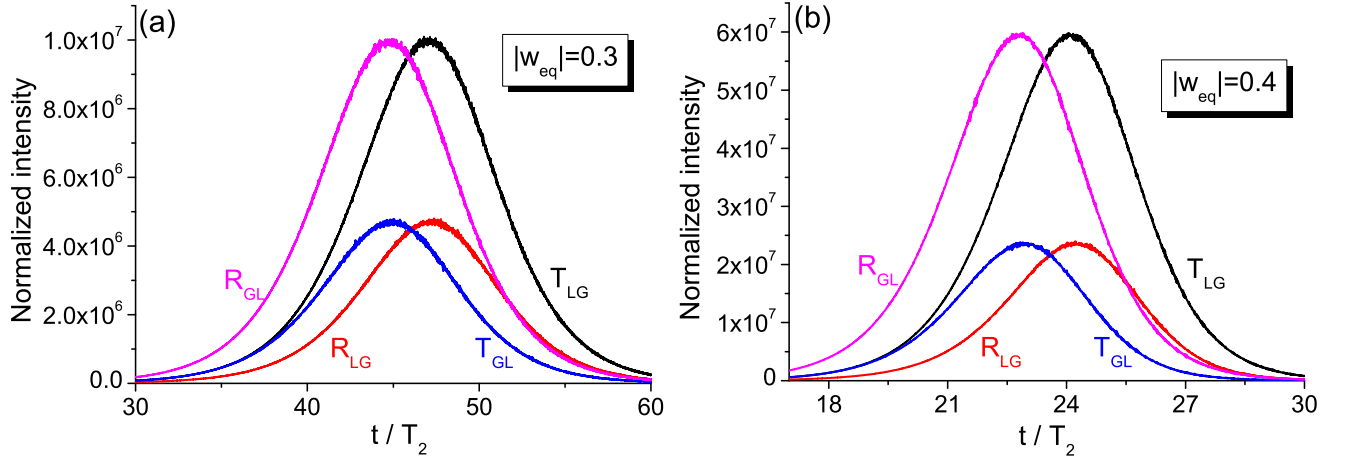
FIG. S1. Temporal dynamics of the reflected (R) and transmitted (T) intensity for the pumping parameter (a) $|w_{eq}| = 0.3$ and (b) $|w_{eq}| = 0.4$.
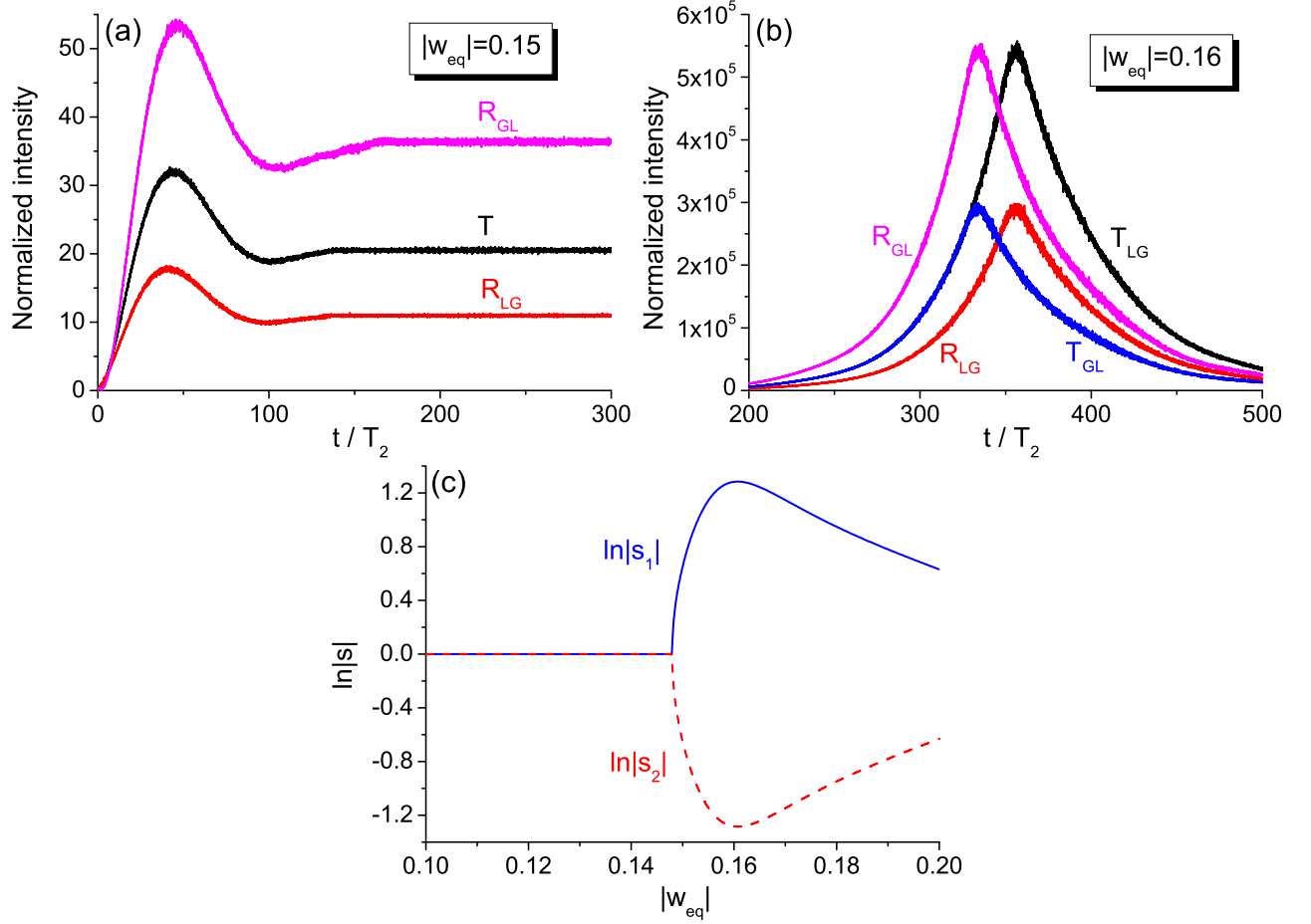

FIG. S2. The case of increased particle density ($\omega_L = 1.5 \times 10^{11}$ s^{-1}): Temporal dynamics of the reflected (R) and transmitted (T) intensity for the pumping parameter (a) $|w_{eq}| = 0.15$ and (b) $|w_{eq}| = 0.16$. (c) Corresponding dependence of logarithm of the scattering-matrix eigenvalues s_1 and s_2 on the pumping parameter. The eigenvalues are calculated with the transfer-matrix method in stationary approximation.
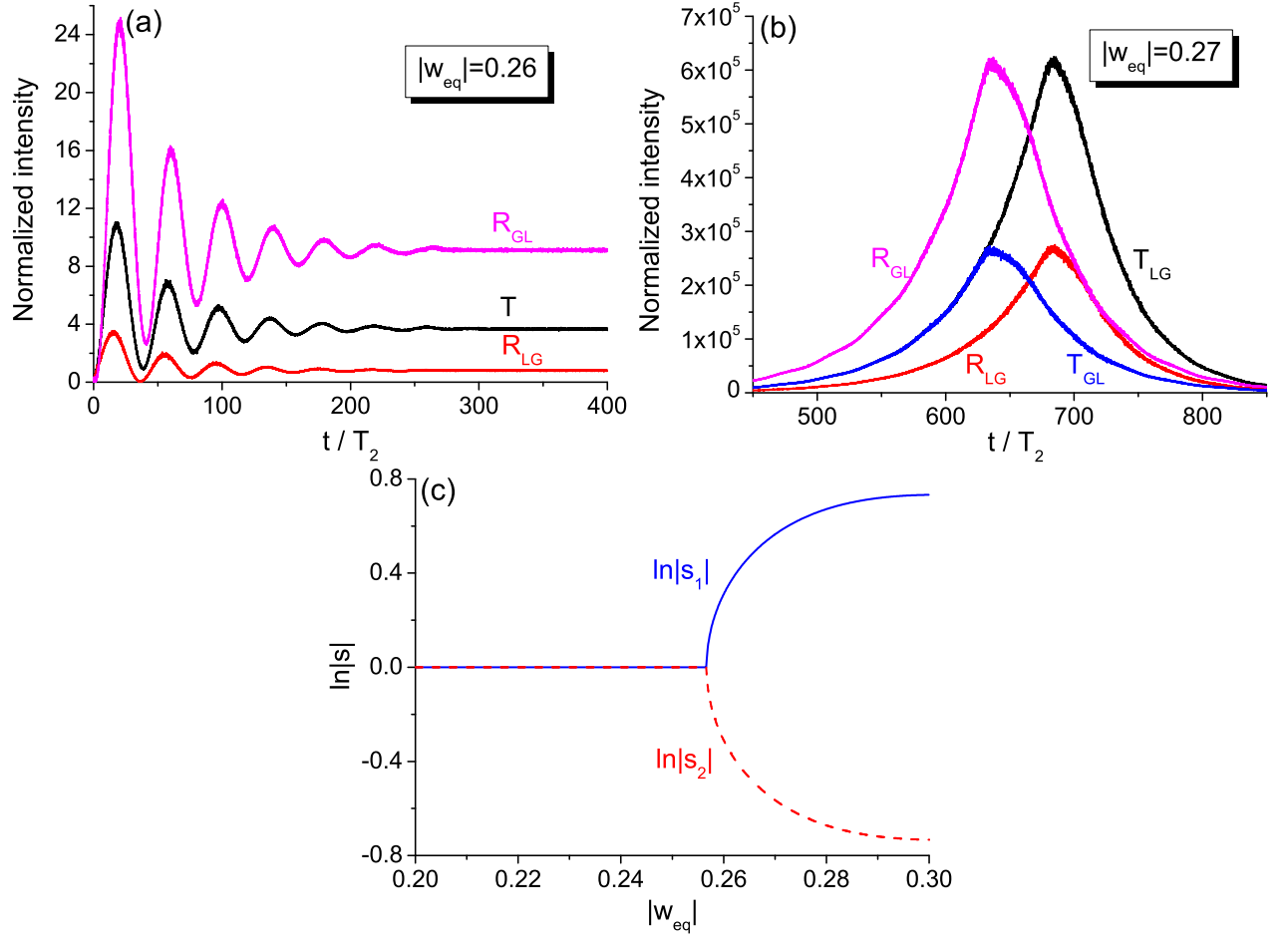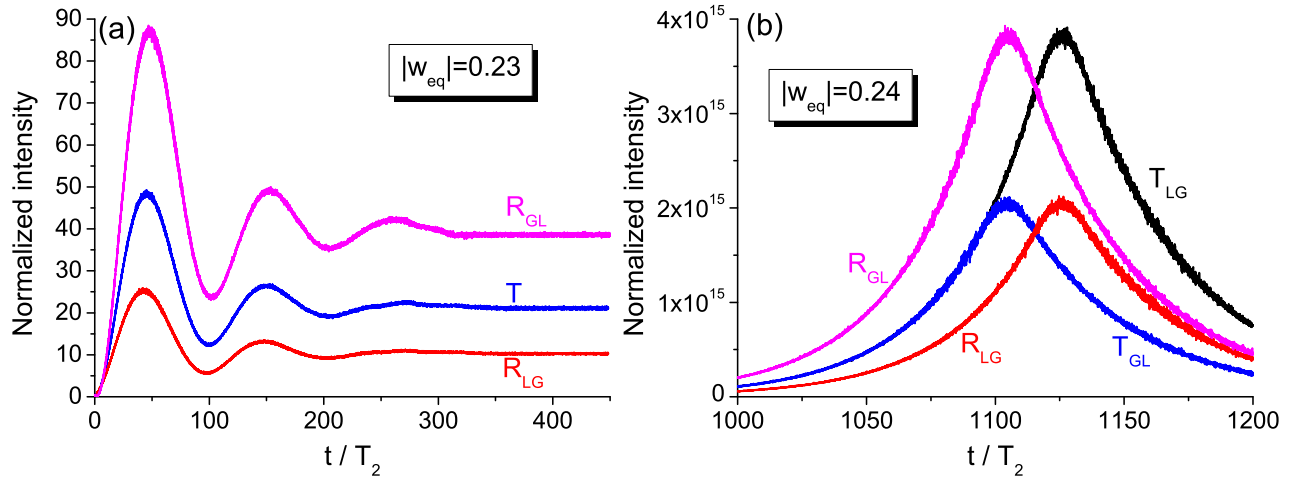
FIG. S3. The case of decreased number of layers ($N = 15$): Temporal dynamics of the reflected (R) and transmitted (T) intensity for the pumping parameter (a) $|w_{eq}| = 0.26$ and (b) $|w_{eq}| = 0.27$. (c) Corresponding dependence of logarithm of the scattering-matrix eigenvalues s_1 and s_2 on the pumping parameter. The eigenvalues are calculated with the transfer-matrix method in stationary approximation.

FIG. S4. The case of lower input intensity $\Omega_0 = 10^{-10}\gamma_2$: Temporal dynamics of the reflected (R) and transmitted (T) intensity for the pumping parameter (a) $|w_{eq}| = 0.23$ and (b) $|w_{eq}| = 0.24$.
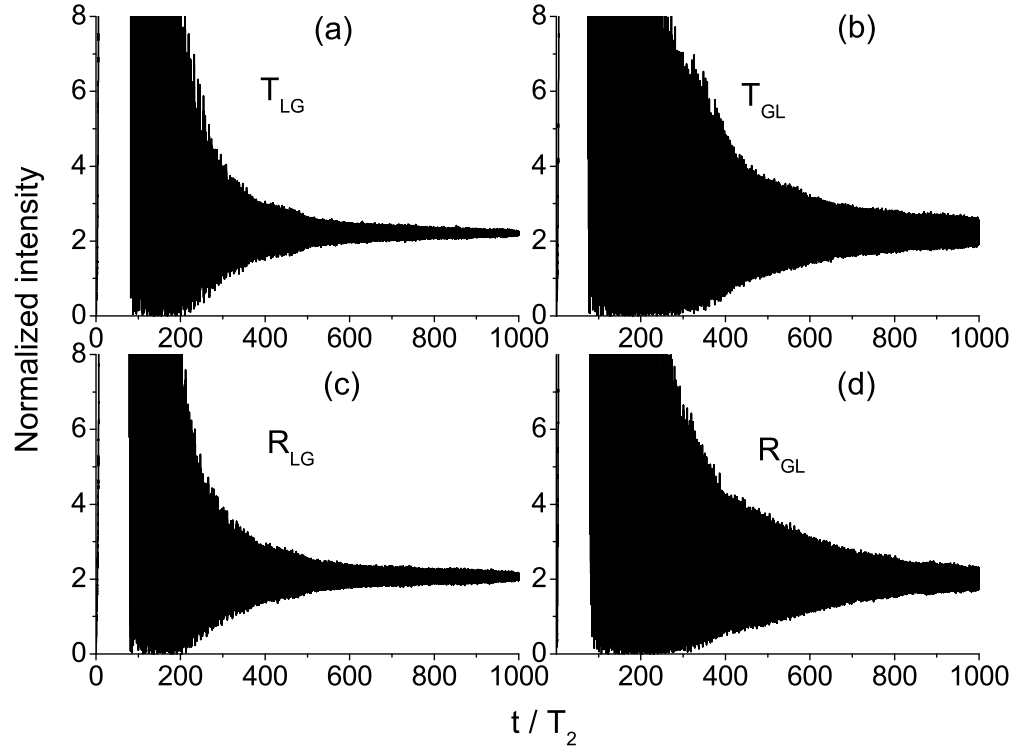
FIG. S5. Stationary state establishment for $|w_{eq}| = 0.3$ [see Fig. S1(a)].
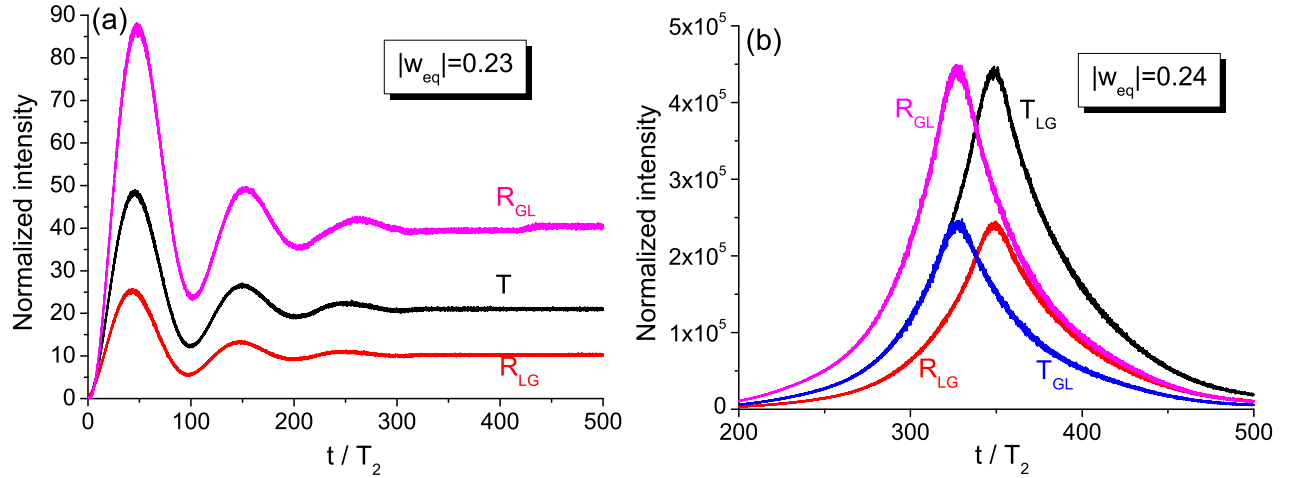

FIG. S6. The case of completely unexcited absorbing layers: Temporal dynamics of the reflected (R) and transmitted (T) intensity for the pumping parameter (a) $|w_{eq}| = 0.23$ and (b) $|w_{eq}| = 0.24$.